Proceedings of the IEEE International Electric Machines and Drives Conference (IEMDC'99), pp.502-504, Seattle, Washington, 1 May 9-12, 1999.

Hybrid Electric Vehicle with Permanent Magnet Traction Motor: A Simulation Model

Levent U. Gökdere, Khalid Benlyazid, Enrico Santi, Charles W. Brice, and Roger A. Dougal

Department of Electrical & Computer Engineering
University of South Carolina
Swearingen 3A80
Columbia, SC 29208
U.S.A.
E-mail: gokdere@ece.sc.edu

Abstract - A simulation model for a hybrid electric vehicle is developed. Permanent magnet synchronous motor is considered for the drive part of the hybrid electric vehicle which comprises three energy sources: (i) a fuel cell, (ii) a battery bank, and (iii) a super capacitor. Rotor-oriented speed controller is designed, and also verified by simulation results, to achieve trajectory tracking requirements of the hybrid electric vehicle within the inverter voltage and current limits.

I. INTRODUCTION

In recent years, hybrid electric vehicles (HEVs) have received much attention as a replacement for high-emission gasoline/diesel engine in cars, buses, and trucks. The main purpose of the use of HEVs is to decrease the urban air contamination especially caused by black smoke, hydrocarbons, and nitrogen oxides of diesel engine in buses and trucks [1].

The electric part of the HEV considered in this paper is composed of (i) three energy sources, (ii) DC-to-DC power converters to control the power into and out of those sources, (iii) a PWM inverter-fed three-phase permanent magnet synchronous motor (PMSM) with associated vector (rotor-oriented) controller, and (iv) a common DC bus.

Fig. 1 shows the block diagram for the electrical part of the HEV. The mathematical models describing the dynamic behavior of each part are given in the following sections.

II. ENERGY SOURCES FOR HEV

There are basically three energy sources to power the HEV. These are (i) a fuel cell for the average power requirements of the HEV (about 10 kW), (ii) a battery bank which provides enough power for hill climbing (about 25 kW), and (iii) a super capacitor for the peak power up to 50 kW for acceleration to a speed of 27 meters per second (60 miles per hour) in less than 10 seconds.

In this work, the relationship between the voltage and the current of the fuel cell is defined as

$$V_{fc} = V_{fcmax} - (V_{fcmax} - V_{fcmin}) I_{fc} / I_{fcmax} \qquad (1)$$

where V_{fc} is the voltage at the terminals of the fuel cell, and I_{fc} is the current flowing out of the fuel cell. In (1), V_{fcmax}=100 V and V_{fcmin}=80 V are the maximum and minimum values of V_{fc}, respectively, while I_{fcmax}=20 A is the maximum value of I_{fc}. The fuel cell provides just enough power to overcome average air drag and other losses at highway speeds. The structure of the fuel cell is described in [2].

The battery bank is composed of a series connection of ten twelve-volt batteries, each rated at 25 Amp-hours. The dynamic equations of each battery are given by

$$V_{charge} = 10.8 + (13.6 - 10.8) Q / Q_{max} \qquad (2)$$

$$V_{terminal} = V_{charge} - R_{internal} I_{battery} \qquad (3)$$

$$Q = \int_0^t (-I_{battery}) dt + Q(0) \qquad (4)$$

where V_{charge} is a non-physical voltage proportional to the state of charge of the battery (Q), $V_{terminal}$ is the voltage measured at the terminals of the battery, and $I_{battery}$ is the current flowing out of the battery. In (2)-(4), Q_{max}=25 Ahr ≈ 90000 coulombs is the maximum charge that the battery can accept, $R_{internal}$=0.015 Ω is the equivalent series resistance of a single battery, and $Q(0)$ is the initial charge of the battery.

The characteristic of the super capacitor used for the HEV is described by the standard capacitor equation:

$$I_{cap} = C \frac{dV_{cap}}{dt} \qquad (5)$$

where V_{cap} is the voltage across the terminals of the super capacitor, I_{cap} is the current flowing into the super capacitor and C=5 farads is the capacitance value of the super capacitor. The super capacitor is able to supply (or accept) the energy necessary for rapid acceleration (or rapid braking).

One objective of this work is to study tradeoffs between sizes of fuel cell, batteries, and super capacitor. The sizes

given are not optimized, but are chosen strictly for the purpose of illustration.

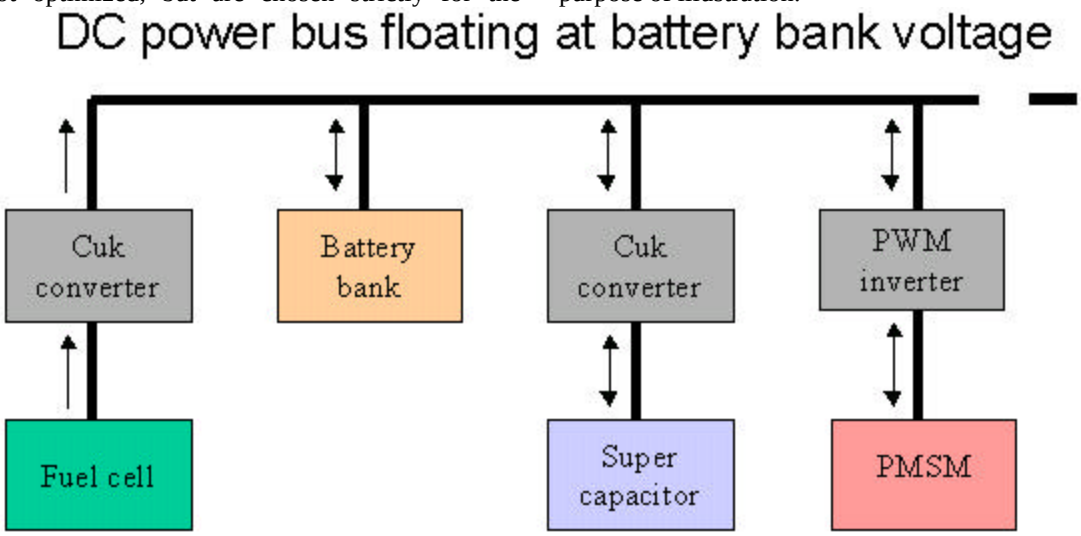

Fig. 1. Block diagram for the electrical part of the HEV.

III. Power Converters

To achieve the desired power transfer between the energy sources and the common DC bus, Cuk type DC-to-DC power converters are utilized (A detailed description of the controllers for the Cuk converters is given in [3]). The fuel cell always supplies the DC bus, and hence, the corresponding Cuk converter is uni-directional. On the other hand, the Cuk converter associated with the super capacitor is bi-directional so that during deceleration, part of the energy released by the motor can be fed into the super capacitor. In this work, the DC bus is assumed to be floating at the battery bank voltage. That is, the batteries are connected directly across the DC bus and there is no intermediate power converter between the batteries and the DC bus.

A three-phase PWM inverter is utilized to drive the PMSM. In the simulation of HEV, an average model of the three-phase PWM inverter is used. The average model is obtained by directly using the calculated values of the stator phase voltages. Also, to be consistent with the practical applications, the inverter voltage and current limits are taken into account.

IV. Drive Motor for Hev

The most common ac motor type used in the electric vehicles (EVs) is the induction motor due to its low-cost, ruggedness, and reliability (see [1] and [4] for the use of induction motors as drive in the EV). However, in recent years, permanent magnet motors tend to replace induction motors in many applications. This is due to the fact that permanent magnet motors have higher torque-to-volume ratio as compared with the induction motors. Also, the decrease in the manufacturing cost of permanent magnets makes the permanent magnet motors appealing. In this paper, taking these factors into account, a three-phase PMSM is proposed for the drive part of the HEV.

The current-command rotor-oriented speed control (vector control) of PMSM is implemented to achieve the acceleration and deceleration requirements of HEV within the inverter voltage and current limits (see [5] and [6] for the basics of the rotor-oriented control of PMSM).

To design, and also test, the current-command rotor-oriented speed controller for the PMSM, a simple vehicle model is used [7]. Specifically, the force opposing the motion of the vehicle consists of three components. These are (i) rolling resistance $F_R = k_R mg\cos q_h$, (ii) aerodynamic resistance $F_A = \frac{1}{2} r C_d A_f \mathrm{v}^2$, and (iii) climbing force $F_C = mg\sin q_h$ where q_h is the angle of vehicle to horizontal and v is the speed of the vehicle [7]. The reference stator current vector in the *d-q* reference frame is then chosen as

$$i_{dq}^* \stackrel{\Delta}{=} \begin{bmatrix} i_d^* \\ i_q^* \end{bmatrix} \stackrel{\Delta}{=} \begin{bmatrix} 0 \\ \frac{1}{p\, l_{max}} (k_0 + k_1 w^2 - k_2 k_p (w - w^*)) \end{bmatrix}$$

where p is the number of pole-pairs, l_{max} is the amplitude of the flux linkage due to the permanent magnets, k_p is the proportional feedback gain, w is the angular velocity of the motor and w^* is the reference value of w. In the reference stator current vector, k_0, k_1, and k_2 are related to the force opposing the motion of the vehicle and are defined as

$$k_0 \stackrel{\Delta}{=} \frac{1}{nh}(mgr_w \sin q_h + k_R mgr_w \cos q_h)$$

$$k_1 \stackrel{\Delta}{=} \frac{rC_d A_f r_w^3}{2n^3 h}$$

and

$$k_2 \stackrel{\Delta}{=} J_m + \frac{mr_w^2 + J_w}{n^2 h}$$

where m=1260 kg is the mass of the vehicle, n=7.3 is the overall gear ratio, h =0.9 is the transmission efficiency, r_w=0.256 m is the wheel radius, k_R=0.009 is the rolling resistance coefficient, r =1.225 kgm^{-3} is the air density, C_d=0.315 is the drag coefficient, A_f=1.75 m^2 is the frontal area, J_m=0.0355 kgm^2 is the moment of inertia of the drive motor (PMSM), and J_w=0.004 kgm^2 is the moment of inertia of the wheels [7].

The controller for the PMSM was designed to provide speed control. But, it can easily be modified to achieve torque control.

V. Simulation Results

Fig. 2 shows the speed tracking performance of the vector controlled PMSM. In this figure, due to the close tracking, the actual and reference speeds are on top of each other. The torque current (i_q) and the DC bus voltage (V_{bus}) are given in Fig. 3. It is seen that during the acceleration phase (from 0 to 10 seconds), V_{bus} drops as i_q increases. On the other hand, in the deceleration phase (from 15 to 25 seconds), V_{bus} reaches a peak value. During the deceleration, the energy released by the motor charges the battery bank via the DC bus. As a result, the DC bus voltage, which is floating at the battery bank voltage, increases. A simulation study, which examines in detail the dynamics of each component in the electrical part of HEV, is presented in [3].

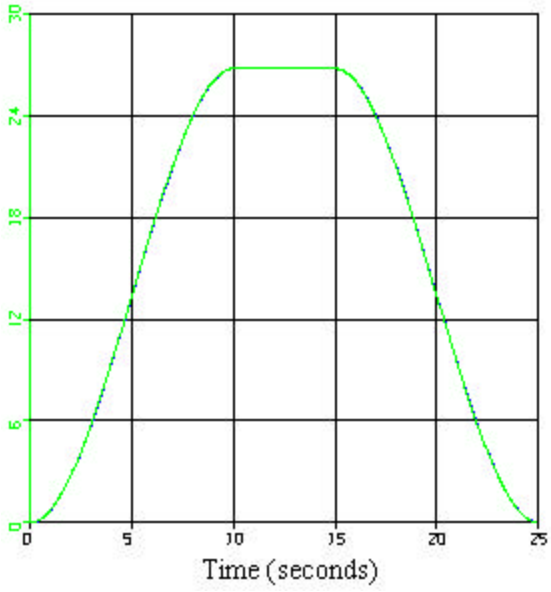

Fig. 2. Actual and reference speeds in meters per second.

VI. Conclusions

A simulation model for a hybrid electric vehicle with vector controlled permanent magnet traction motor is developed and also verified. In the simulation, linear models for the energy sources (fuel cell, batteries, and super capacitor) are used. The future work will incorporate more accurate models of the energy sources in the simulation.

Acknowledgment

This work was supported in part by the Office of Naval Research under Grant N00014-96-1-0926.

References

[1] H. D. Lee and S. K. Sul, " Fuzzy-Logic-Based Torque Control Strategy for Parallel-Type Hybrid Electric Vehicle," *IEEE Transactions on Industrial Electronics*, vol. 45, no. 4, pp. 625-632, August 1998.

[2] T. Gilchrist, " Fuel Cells to the Fore," *IEEE Spectrum*, pp. 35-40, November 1998.

[3] K. Benlyazid, L.U. Gökdere, E. Santi, C.W. Brice and R. Dougal, "Hybrid Electric Vehicle: A Simulation Study," *Proceedings of IASTED Conference on Modelling and Simulation (MS'99), Philadelphia, PA,, May 5-8, 1999.*

[4] J. Jung and K. Nam, " A Vector Control Scheme for EV Induction Motors with a Series Iron Loss Model," *IEEE Transactions on Industrial Electronics*, vol. 45, no. 4, pp. 617-624, August, 1998.

[5] P. Vas, *Vector Control of AC Machines*, Oxford, U.K.: Clarendon Press, 1990.

[6] W. Leonhard, *Control of Electric Drives*, Berlin, Germany: Springer-Verlag, 1985.

[7] A. Harson, P. H. Mellor, D. Howe, " Design Considerations for Induction Machines for Electric Vehicle Drives," *Proceeding of IEE Seventh International Conference on Electric Machines and Drives*, University of Durham, U.K., September 11-13, 1995, pp. 16-20.

Proceedings of the IEEE International Electric Machines and Drives Conference (IEMDC'99), pp.502-504, Seattle, Washington, 4 May 9-12, 1999.

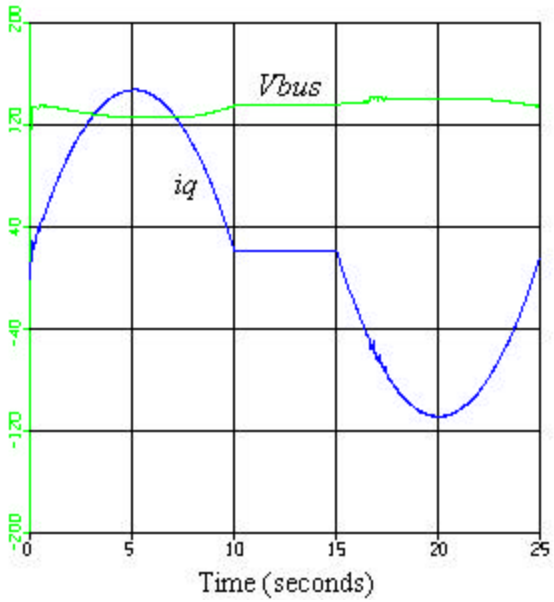

Fig. 3. Torque current in amperes and bus voltage in volts.